

ISSN 2063-5346



# RECENT DEVELOPMENTS AND RESEARCH PROGRESS IN WELDING OF INCONEL ALLOYS WITH DISSIMILAR ALLOYS-A REVIEW

Fasil T Mohammed<sup>1</sup>, Dr. Mohammad Nizamuddin Inamdar<sup>2</sup>

---

Article History: Received: 01.02.2023

Revised: 07.03.2023

Accepted: 10.04.2023

---

## Abstract

Welding techniques are one of the most critical and often used methods for joining pieces in the different industries. Stainless steels are widely accepted alloys in industry. But corrosion resistance and heat resistance capability are not excellent as Inconel. Inconel alloys are highly useful for extreme heat resistance, superior mechanical strength and corrosion-resistant applications in aerospace, petrochemical, oil and gas industries. Combining Inconel with other alloys, such as stainless steel, is an efficient idea to reduce its cost drastically. This paper discusses different approaches used in industry to combine Inconel with different alloys. Welding, cladding and overlaying are the most effective methods to join Inconel with other alloys. Inconel 718 and Inconel 625 have undergone a comparatively high number of studies, which seems practical to join with different alloys. High grades of Inconel alloys have undergone less number of dissimilar welding studies.

**Keywords:** Welding, Inconel Alloys.

---

*Research Scholar 1, Associate Professor2, Faculty of Engineering and Built Environment,  
Lincoln University College, Malaysia.*

*ftmohammed@lincoln.edu.my, nizamuddin@lincoln.edu.my*

**DOI:10.31838/ecb/2023.12.s1-B.381**

## INTRODUCTION

Inconel alloys are a type of nickel-based superalloys known for their exceptional corrosion resistance and high-temperature strength [1]. Due to the expensive nature of Inconel, it is not cost-effective to use Inconel completely for industrial requirements. Not suitable as Inconel, stainless steel is also a good option in corrosive conditions. High temperature components, aircraft engines, and the nuclear power industry all make use of stainless steels and Ni alloys [2-4]. Also for getting the advantage of Inconel alloy, it is widely using as overlaying material over different alloys. [31,35,39] Dissimilar joints are crucial for some applications that must function at high temperatures. Dissimilar welding of Inconel to stainless steel has been widely used in the design and fabrication of a wide variety of structural compounds for both cost-saving and performance-improving reasons. Welding two alloys together that have different melting points and thermal expansion coefficients is difficult. Combining Inconel (Ni-based superalloys) and SS is of interest to scientists for usage in corrosive and elevated temperature environments. By effectively employing each material, i.e., using each material's unique capabilities, joining different metals opens up possibilities for the product's flexible design. Oil refineries, power plants, chemical and petrochemical industries, nuclear power plants, aerospace, onshore and offshore, and other technical applications take use of its low cost and adaptable design. [5-10]

### I. LITERATURE REVIEW

Vivek Patel et al conducted Electron Beam welding (EBW) on rolled Inconel 718. The results of the tests demonstrated that the heat input was proportional to the weld penetration depth and fusion area, and a microhardness measurement revealed a softer and larger weld zone at the beam inlet after welding. Both of these findings were based on the finding that the weld penetration depth and fusion area were proportional to the heat input. If gaps are found at the base of welds when using the maximum beam power of 3250 watts and scanning speeds more than 0.78 m/min, they can be removed with the use of an appropriate machining operation. The ductility (57%) of the welded specimen also met the specs when the welding heat input was less than 225 J/mm. With modest heat inputs, the welded samples fractured outside the weld area, revealing the outstanding weld strength and durability. The welded samples all cracked and broke where they were welded when the heat input was increased. [11]

P. Thejasree et al investigated laser beam welding of Inconel 625 and came to the following conclusions. Keyhole weld structures form at weld speeds of 5mm/s with heat input of 100W or greater. Additionally, it was discovered that less heat input leads to smaller grains, which increase mechanical characteristics and result in a reduced heat-affected zone because of very fast cooling. The measured value of UTS was to be 1290 MPa with 20% elongation, as well as 1370 MPa with 30.9% elongation. The combined ultimate strength of 3.01% of yield stress and 1597.22MPa is 1600MPa. It was discovered that as the intensity of the laser beam was raised, the melt zone grew in both width and depth. The metal being welded experiences the greatest temperature differential near the heat source and gradually cools away from it when the heat source recedes from it. [12]

Thin sheets of Inconel 625 and Duplex stainless steel 2205 were Ytterbium fiber laser welded experimentally by Gulshad Nawaz Ahmad et al. They were successful in producing joints constructed of inconel 625 and DSS 2205 that had strong bonds, were homogeneous, and included no defects. The weld joint's heat input was a key factor in determining the bead form. Higher energy input led to the formation of top glass shapes and X-shaped beads, while lesser energy input resulted in the formation of V-shaped beads. When heat was applied, the weld metal's microstructure showed multidirectional grain development with cellular and columnar dendritic at high temperatures and much finer cellular and columnar dendritic at low temperatures. The interdendritic region of the weld metal displayed segregation of MO, Nb rich phases according to EDS analysis, which also revealed that the weight % of segregation is highest at heat input of 43 J/mm. Austenite precipitates and laves were discovered by phase analysis. A micro-hardness analysis of the weld metal showed that when heat input decreased, the hardness value increased as a result of finer dendritic grains and smaller dendritic arm spacing. Failure occurred in the parent material of DSS2205 and the maximum failure strength of dissimilar joints was determined to be 890Mpa for S4 (21.5 J/mm), which is larger than the strength of DSS2205. [13]

A study on microstructural change during laser welding of Inconel 718 was undertaken by Sumit K. Sharma et al. The weld zone contains reinforcement, which ranges in size from 51.3 micrometers to 70.9 micrometers and gets bigger as the scan speed goes up. Weld zone area reduces as scan speed increases, with the smallest weld zone area seen for the scanned sample at 1400mm/min. Precipitates are present in the interdendritic region of the weld zone, which has a mostly dendritic morphology. Welding creates a seamless and flawless solid-liquid contact by creating and fostering the growth of columnar grains at the interface. Laser welding reduces the lattice strain in Inconel 718 from 0.39 as received to 0.19 to 0.33 depending on the scan speed. Because of laser welding, the microstructure has become more uneven, and the average grain size is now 47.6 micrometers, which is significantly larger than the 20.5 micrometers that were present in the Inconel 718 when it was first acquired. When Inconel 718 is laser welded, the KAM angle is observed to be somewhat lowered from 0.53 to 0.51. [14]

J. Sivakumar conducted study on the systematic welding process parameters optimization in activated tungsten inert gas (A-TIG) welding of Inconel 625. When compared to the parameter set from TOPSIS, it was found that the parameter set that was acquired through the use of GRA was more closely aligned with the results of the experiments. It was discovered that the arc gap should be 5 millimeters, the torch speed should be 90 millimeters per minute, and the current should be 300 amperes for the method of welding to work well. According to the findings, the penetration was 6.5 millimeters, the weld cross-sectional area was 65.55 millimeters squared, the microhardness was 271.5 hV, the bead width was 19.5 millimeters, and the bead height was 0.1 millimeters. The outcomes showed that a multicriteria decision-making technique could significantly increase weld quality, as shown by the grey relational grade value. Additionally, it should be highlighted that using an activating flux and a higher welding heat input led to deeper penetration. When microhardness tests were done, it was found that the area around the weld had a higher

microhardness than usual. This was because the A-TIG weld method had a high energy content and a delayed cooling rate. Due to ongoing A-TIG welding, the weldment zone has enriched Ni, according to XRD measurements. The weld puddle would be able to withstand oxidation, corrosion, spalling, and wear. [15]

Modelling and experimental validation of TIG welding of inconel 718 has been conducted by S. Tamil Prabhakaran et al. Both the FE model and the actual work recorded high temperatures of 453° C and 442° C, respectively, on the central surface, 6 mm from the center line of the weld. This was done so that at the quasi-steady state, there would be very little temperature variation in the process. Conditions in the heat cycles are consistent with expectations. When the system is in a quasi-steady state, the predicted and observed fusion zone shapes and sizes agree well. The top surface of the FZ has a half width of 1.4 mm, the middle plane has a half width of 1.35 mm, and the bottom surface has a half width of 0.95 mm. Half-width measurements from a real weld are 1.59 millimeters on the top surface, 1.17 millimeters in the middle plane, and 0.82 millimeters on the bottom surface, therefore these results are quite favorable. Half widths for FZs and HAZs on the top surface were expected to be 1.4 mm and 0.63 mm, 1.35 mm and 0.66 mm, and 0.95 mm and 0.85 mm. Specifically, INCONEL 718 HAZ is prone to heat cracking between 1225 and 1327 C, just around the fusion line, which is close to the 1327 C isotherm. The center line of the weld is projected to be 1.375 mm away from the vulnerable hot crack zone's location and width. [16]

Ateekh Ur Rehman et al welded Inconel 718 to Inconel 600 by rotary friction welding. Through the use of rotary friction welding, inconel 718 and inconel 600 may be easily welded together. There were no difficulties with cracking at any of the welds. Additionally, the welds lacked Laves forms and unwanted elements segregation. The HAZ of either Inconel 718 or Inconel 600 did not experience any microstructural changes that were deemed to be significantly undesirable as a result of friction welding. But along the weld contact, both alloys had some grain coarsening. A small mechanical intermixing zone at the contact distinguished the dissimilar weld. Extremely high temperatures and plastic deformation in this zone led to dynamic recrystallization, which produced incredibly small equiaxed grains. As a result, this area showed noticeably enhanced hardness. Dissimilar friction welds between Inconel 718 and Inconel 600 showed exceptional room temperature tensile properties in their as-welded form. The weld in the Inconel 718 heat affected zone failed as a result of substantial grain coarsening. [17]

Yahya Aghayar et al done an assessment of microstructure and mechanical properties of inconel 601/304 stainless steel dissimilar weld. Studies using a high vacuum FE-SEM showed that the weld metal had not segregated. It was discovered that a reduction in the amount of heat input caused substantial refinement of grains in the welds, which resulted in an improvement in the mechanical properties of the welds. Pulsed current welding produced welds with superior mechanical characteristics as compared to those made with filler metals. Autogenous welding resulted in the production of a product that had an extraordinary strength-ductility relationship (UTS = 485 MPa and the elongation = 39%). [18]

A study has been done on microstructure and mechanical properties of combined GTAW and SMAW dissimilar welded joints between Inconel 718 and 304L austenitic stainless steel by Sachin Sirohi et al. Study of the microstructure revealed the emergence of an unmixed area on the 304L side of the stainless steel. The microstructure of the weld metal showed that it was entirely austenitic, with phases of Nb- and Ti-rich carbide in the spaces between the dendrites. After being subjected to tensile testing at room temperature, the welded metal was found to have fractured. This was most likely due to the fact that the alloying components were dispersed along the intervals in between the dendrites. However, at 600 C, tensile testing showed that the 304L stainless steel base metal failed, with values of 377 MPa and 24% in elongation and tensile strength, respectively. The hardness plot reveals that the mean hardness value of the weld metal is 236 5 HV. This value is higher than the 204 4 HV of the 304L SS BM but is lower than the 243 5 HV of the IN718 BM. The hardness of the welding metal was only 109 J, which indicates that it is significantly less robust than base metals. It's possible that the NbC phase formed along the interdendritic voids, which would explain why the weld metal has poor impact strength. [19]

M. Paidar et al conducted a study on diffusion brazing of Inconel 617 and 321 stainless steel by using AMS 4772 Ag interlayer. Ag's capillarity effect allowed for the creation of void-free diffusion-brazed joints, and a longer brazing/holding period produced a joint with a more uniform reaction layer. A joint that was brazed for 60 minutes had a maximum shear strength of 322.9 MPa, which was 26% higher than a joint that was processed in 30 minutes. The low shear strength of the sample obtained after 30 minutes of brazing and holding was due to the material failing mostly in a brittle (fracture) manner. The AMS4772 Ag interlayer has been used to successfully link the IN617 and AISI 321 SS alloys at a sufficient brazing/holding duration. [20]

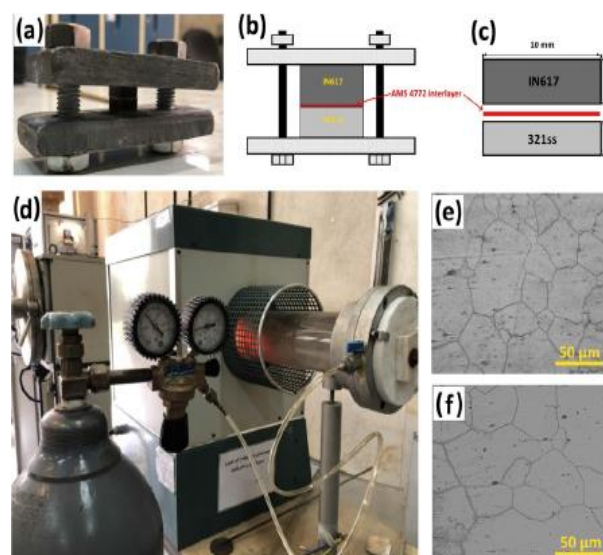


**Fig. 1.** Diffusion brazing process and microstructure (a) special fixture for the clamped materials arrangement, (b) and (c) illustrations of the clamping and materials arrangement, (d) furnace used for the process, (e) microstructure of AISI 321 SS, (f) Inconel 617 [20]

Muralimohan Cheepu et al conducted an experiment on laser welding of dissimilar alloys between high tensile steel and Inconel alloy for high temperature applications. On the side that was made of Inconel 718, microstructural characteristics, the presence of precipitates, and the development of martensite on the high-tensile steel were observed. Experiments with EDS and EPMA showed the existence of "strengthening precipitates" as well as the interdiffusion of elements along the edges of grains. On both substrates, the microhardness rose and approached the HAZ. The precipitates in Inconel 718 were responsible for the rise, while martensite was responsible for the increase in high-tensile steel. At a laser power of 1.5 kW, the joints attained their maximum strength of 672 MPa; however, as the laser power was increased, the joints' strength started to diminish. In light of the fact that there were only a few brittle zones, fractography was used to investigate the ductile mode of failure. [21]

A. K. Sahu et al investigated on mitigation of micro-cracks in dissimilar welding of Inconel 718 and austenitic stainless steel. With pulsed  $\mu$ -PAW welding, a reasonable level of joint strength and ductility between Inconel 718 and SS316L has been achieved. When welding was done at a high rate (196 mm/min), the whole weld bead had a columnar dendritic pattern. When welding was done at a low rate (145 mm/min), the structure was equiaxed. Because there are more Nb, Mo, and Ti where there are microfissures and microcracks in the solidification, it looks like an intermetallic layer may have formed there. Analyses using X-ray diffraction revealed the existence of intermetallic phases in the weld zone. These intermetallic phases included NbC, Laves (Fe<sub>2</sub>Nb), and TiC. The microstructural morphology shifts from a continuous columnar dendritic structure to an equiaxed dendritic structure if the level of weld dilution is increased while the welding speed is slowed down at the same time. There is a slight decrease in the micro-hardness of the material in the welded zone whenever the rate of welding is slowed down. When the pace of the welding process is slowed down, the elongation of the welded component climbs to 90%, despite the fact that the tensile strength of the part is enhanced quite a bit. [22]

Fatigue analysis of Ti6Al4V/INCONEL 625 dissimilar welded joints has been researched by Pasqualino Corigliano et al. As a result of the difficulty involved in making a direct connection between titanium and inconel, plates with inserts made of vanadium and AISI 304 steel were produced to measure 200 millimeters in length. The results of the testing showed a fatigue strength of 159 MPa, which validated the good quality of the joint that was tested. The fatigue strength that was found was looked at and compared to that of other joints that had been welded with similar shapes and were made from the same base materials. When compared to homogenous welded joints made of AISI 304 and Ti6Al4V (as welded) samples and vanadium fatigue strength, Ti-Inconel joints made during this study were found to be of higher quality. This conclusion was reached after comparing the joints to determine their quality level. The infrared (IR) approach was applied in order to keep an eye on the weld, and the results demonstrated that it was successful in detecting the crack's hot area. Additionally, the TM was utilized, and its fatigue strength value matched that of traditional fatigue testing, verifying its application for the aforementioned welds. [23]

This work employs micro structural analysis for Nd:YAG pulsed Wave mode welding samples both before and after heating. The Nd:YAG pulsed Wave mode welding takes into account a variety of variables, including laser power, welding speed, and frequency. When doing microstructural analysis for the purpose of pre-heating welding samples, the heat generated by the welding process has an effect on the parent metal grains located at the fusion zone. The heat from the welding process does not affect the original metal grains at the fusion zone, and the structure of the grains in the welded area is only slightly modified after being subjected to post-heating welding samples. This work's conclusions come from post-heat treatment processing, which may boost ductility and tensile strength. This work may help fabrication firms cut down on experimentation's expense and time. [24]

Microstructure characterization in Dissimilar TIG welds of inconel alloy 718 and high strength tensile steel conducted by M. Anuradha et al. Precipitates are generated along the site of fusion between the area of welding and the Inconel 718 alloy, which is the location where the microstructure may be observed. The section of Inconel 718 known as the fusion border has a higher hardness than both the base metal and the fusion zone. On the other hand, the region of high-tensile steel known as the heat-impacted region has the highest hardness. The strength of the joints was compromised at the weld zone and the filler metal deposition, both of which are robust in their own right but are not as strong as the joints themselves. According to the results of the element line scan analysis, the weld zone and the region along the fusion boundaries of the Inconel alloy both generated Nb- and Ti-rich precipitates.. [25]

Microstructure and mechanical properties for the dissimilar joining of Inconel 718 alloy to high-strength steel by TIG welding were researched by M. Anuradha et al. Within the weld and the dendritic structure that is located close to the fusion boundaries, an extremely fine and equiaxed dendritic microstructure is produced. This takes place in the middle of the dendritic structure as well as the weld. At the AISI4140 fusion border, no precipitates are seen, and the microstructure is martensitic. In the Inconel 718 fusion line, a few precipitates are present. An EDS line scan and an EPMA mapping study both point to the creation of c0, c00, and NbC in the weld metal. Both of these results may be seen. According to the microhardness patterns and mapping profiles, the weld region has a softer texture than the interdendritic precipitation, which has a rougher texture. The interdendritic precipitates have a higher hardness. The weld zone and the Inconel 718 fusion borders of the joints fail with a combination of fragile and ductile natures, and the best feasible strength is produced when the welding current is set to 130 A. The failure is due to the joint itself. [26]

Mechanical and microstructural characterizations of friction stir welded dissimilar butt joints of Inconel 718 and AISI 204Cu austenitic stainless steel were studied by Sanjay Raj et al. The results showed that the mechanical properties of the nugget zone got better as M23C6 carbide particles and fine, evenly shaped, restructured austenite and ferrite grains formed. The fact that M23C6 carbide particles were found in the nugget zone showed that these improvements had been made. The atomic diffusion zone of the Inconel 718 and AISI 204Cu joint interface revealed an FCC microstructure with refined MC carbide particles (a median dimension of 40 nm) in addition to NbC carbides. This zone had an average

thickness of 1.5 micrometers. (average size of 50 nm). In addition, it was discovered that Inconel 718, which was dragged on the moving side of the stainless steel 204Cu and connected to the joint's strength, was present. In all circumstances, dynamic recrystallization was seen to refine the grains in the nugget zone, improving their mechanical characteristics. [27]

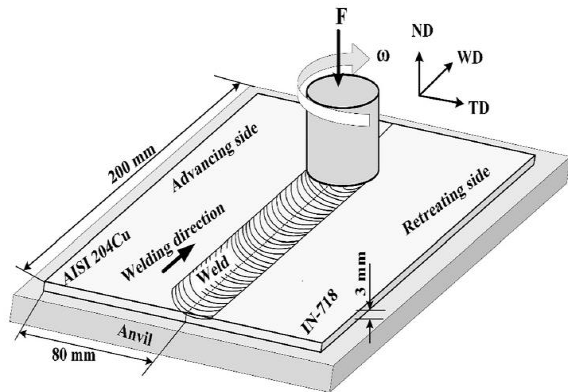


Fig. 2. Schematic diagram of FSW process. [27]

Xipeng Zhao et al conducted a study on improvement in corrosion resistance of wire arc additive manufactured Inconel 625 alloy through heat treatment. The corrosion resistance of the Inconel 625 alloy as deposited was different from that of the wrought Inconel 625 alloy, according to potentiodynamic polarization tests. After heat treatment at 980 °C, the corrosion resistance decreased because the needle-like phases offered more places for pitting to start. The passivation current density ( $I_{corr}$ ) reduced by 52% after heat treatment at 1100 °C, while the corrosion potential ( $E_{corr}$ ) raised by 32%. This result was nearly equivalent to that of wrought Inconel 625 alloy. Recrystallization occurred as a result of the dissolving of laves and phases, the decreasing strength of the 001 orientation, the decline in the number of low-angle boundaries, and the production of a high number of stable twin grain boundaries, according to the findings of an exhaustive microstructural examination. Every one of these occurrences took place at the same time. The astounding corrosion resistance of the 1100 °C heat-treated Inconel 625 was made possible by all the crystal and microstructure evolution. [28]

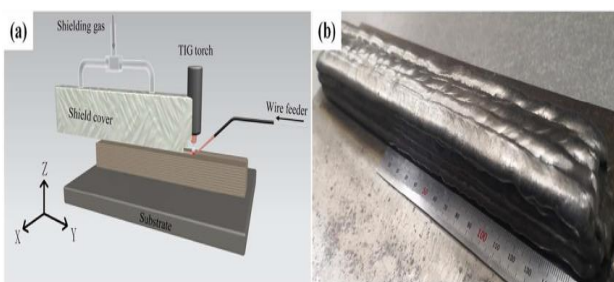


Fig. 3. (a) Experimental setup of the WAAM process; (b) Inconel 625 component fabricated by WAAM. [28]

Camila P. Alvaraesa et al researched on microstructure and corrosion properties of single layer Inconel 625 weld cladding obtained by the electroslag Welding Process. Weld claddings with the right corrosion and microstructure characteristics can be created using ESW at room temperature, and the process also improves productivity significantly. The corrosion results of ESW-produced single-layer weld overlays at room temperature were similar to those of other methods and even some base materials. We were able to accomplish a weld overlay using ESW at distances of 1.0 mm and 3.0 mm from the fusion line. This made it possible for us to make a weld deposit with the right microstructure and corrosion properties. ESW is a great choice for making machinery because it can make single-layer cladding with the right mechanical properties at a high rate. Weld claddings can be made with ESW at room temperature. This method not only increases output by a large amount, but also makes weld claddings with the right microstructure and corrosion properties. At room temperature, corrosion tests on single-layer weld overlays made with ESW gave the same results as those done with other methods and even on some base materials. When ESW was used to make a weld overlay, a weld deposition happened between 1.0 mm and 3.0 mm from the fusion line. The corrosion and microstructure of this weld deposition were right for the job and similar to those of the original weld. ESW is an attractive option for making equipment because it can make a single-layer cladding with the right mechanical properties and at a high rate of production. This makes ESW a viable option for use in industrial gear. [29]

Cleiton C. Silva et al conducted an assessment on microstructure of alloy Inconel 686 dissimilar Weld Claddings. Using EDS, microchemical studies showed that Ni with  $k > 1$  went through microsegregation, which made the dendritic core richer, while Mo with  $k < 1$  went through microsegregation to the liquid. Because the results for W were different from sample to sample, it was hard to figure out what they meant. On the other hand, the results for Cr showed a very minor tendency to separate from the liquid. (k1). The results of the SEM and TEM chemical study of precipitates revealed that the precipitates were made up of Ni, Fe, and Cr and that they were notably concentrated with Mo and W. P-phase, s-phase, and m-phase were found to be the topologically closed-packed TCP phases that were identified by TEM analysis as being based on electron diffraction characteristics in specific regions. [30]

TABLE I  
WELDING METHODS FOR SIMILAR & DISSIMILAR METALS

Work piece	Material 1	Material 2	Welding Method	Ref
Rolled plate	Inconel 718	Inconel 718	EBW	[11]
Plate	Inconel 625	Inconel 625	LBW	[12]
Thin sheets	Inconel 625	Duplex stainless steel 2205	Yterbium LBW	[13]
Plate	Inconel 718	Inconel 718	LBW	[14]
Plate	Inconel 625	Inconel 625	A-TIG	[15]

Plate	Inconel 718	Inconel 718	TIG	[16]
Rods	Inconel 718	Inconel 600	Rotary Friction Welding	[17]
Sheet	Inconel 601	304 Austenitic stainless steel	TIG	[18]
Plate	Inconel 718	304 L	TIG&SM AW	[19]
Plate	Inconel 718	ISI4140	LBW	[21]
Thin sheet	Inconel 718	Austenitic stainless steel	$\mu$ -PAW	[22]
Plate	Inconel 625	T16AL4V Vnadium AISI304	LBW	[23]
Sheet	Inconel 625	Inconel 625	Nd:YAG LBW	[24]
Plate	Inconel 718	AISI4140	TIG	[25]
Plate	Inconel 718	AISI4140	TIG	[26]
Plate	Inconel 718	AISI204Cu	FSW	[27]
Plate	Inconel 625	Inconel 625	TIG	[28]
Plate	Inconel 625	Inconel 625	PCGTA	[37]
Rod	Inconel 713LC	AISI 4140	Nd:YAG LBW	[41]
Sheet	Inconel 601	304 Stainless steel	GTAW	[42]

Lianyong Xu et al were investigated insights into the intergranular corrosion of overlay welded joints of X65-Inconel 625 clad pipe and its relationship to damage penetration. During corrosion tests, IGC showed less resistance as the sample got closer to the X65 side. The weld was particularly susceptible to IGC because the material had a tiny grain size and a high concentration of Fe. Different types of corrosion formed in the base metal (BM) and the heat-affected zone (HAZ) because corrosion went into the material to different depths. (HAZ). As the corrosion immersion test progressed, pitting in the BM transformed into inter-dendritic corrosion. Due to the enhanced grain boundary structure and lower Fe content in the CMT-welds, the IGC resistance of the CMT-welds is significantly higher when compared to the GTAW welds produced by gas tungsten arc welding (GTAW). This increase is noticeable. When the overlay is closer to the X65 substrate, it has a lower resistance to IGC. This takes place as a consequence of the overlay having a high concentration of Fe and having a finer grain size in the region directly above the substrate. [31-32]

A study on microstructural and mechanical characterization of the transition zone of 9%Ni Steel clad with Ni-Based super alloy 625 by GTAW-HW conducted by Francisco Werley Cipriano Farias et al. By looking at the metallography, type I and type II borders were found to have MC-type carbide, Laves/g eutectics, macrosegregation

on peninsulas, a texture of crystals close to 100 $\mu$  in the clads, residual strain, and a decrease in microhardness. This was done throughout the transition zone. The clads are of sufficient quality, as shown by the shear and bend tests that were performed on them. In dissimilar welds of steel, our research indicates a new type II boundary creation mechanism. These welds do not suffer a shift in the solidification mode and do not exhibit an allotropic transformation during the welding heat cycle. [33]

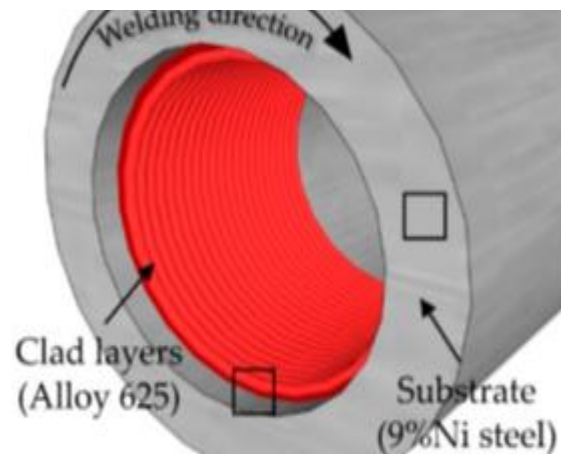


Fig. 3. Schematic representation of 9%Ni steel (ASTM A333 Gr. 8) pipes cladded with one and two layers of Ni-based super alloy 625 (AWS ER NiMoCr-3) [33]

Guo Longlong et al researched on formation quality optimization and corrosion performance of Inconel 625 weld overlay using hot wire pulsed TIG. There are relationships that are both substantial and adequate between the process parameters and the quality of the creation of clad beads. The planner crystals are located at the bottom of the microstructure, followed by cellular dendrites, columnar dendrites in the center, and equiaxed and directing dendrites at the very top. This process can be seen throughout the entire structure. There are flat crystals and dendrites coming from all of the different cells scattered all across the fusion zone. In a comparison of the corrosion performances of the first and second cladding samples, the second layer specimen demonstrates superior results. In addition, the performance of the second layer with regard to corrosion is comparable to that of wrought Inconel 625. The corrosion performance of the weld overlay is negatively impacted when an excessive amount of Fe is present. [34]

P. Elango et al conducted study on welding parameters for Inconel 625 overlay on carbon steel using GMAW. According to the findings of the research, it is not possible to make a reasonable overlay without first ensuring that all of the process variables — all of the parameters, such as ampere, voltage, travel speed, shield gas flow rate, and arc distance, are adjusted to their correct values. It is necessary to have corrosion resistance, which proves that the corrosion characteristics have not been altered in any way. The weld cap has more hardness than the base metal area. What this means is that the weld overlay is more durable and corrosion-proof than the base metal. The weld joint's macrostructure demonstrates that the source material and the

weld overlay have successfully fused together, and there are no further indicators of any anomalies. [35]

Performance of the INCONEL 625 alloy weld overlay achieved by FCAW technique was the subject of research by Camila P. Even though there were secondary phases and PDZ in both the as-welded and stress-relieved conditions, the satisfactory mechanical and corrosion properties found in this study show that the FCAW process is a good way to make nickel-based superalloy Inconel 625 weld overlays. This is because neither the next phases nor the presence of PDZ got in the way of getting the results they wanted. When compared to more conventional methods of production, the improvement stands out. [36]

Pavan Kumar Korrapati et al. done an assessment of mechanical properties of PCGTA weldments of Inconel 625. There may not be any flaws in the successful weldments produced by the PCGTA welding process while using Inconel 625. Welds made with ERNiCrMo-3 and Inconel 625 PCGTA had an average tensile strength of 852.4 HV, and it was found that the tensile strength broke at the weld. Increased amounts of Nb, Ti, and Mo all contributed to the improved mechanical qualities. [37]

Effect of heat treatment on microstructure and mechanical properties of Inconel 625 alloy fabricated by pulsed plasma arc deposition were experimented by Fujia Xu et al. Only the hardening phases and the Ni<sub>3</sub>Nb precipitating phases separated the as-deposited microstructure from the direct-aged (DA) microstructure in terms of hardness and tensile strength. However, due to the existence of the fragile Laves phase, the plastic's properties were subpar. Large amounts of Laves phases were dissolved by the 980 STA treatment, which allowed for the deposition of a needle-like delta phase. The mechanical properties of the sample were enhanced without compromising its ductility. The Laves phase was entirely dissolved after the 1080 HSTA treatment. However, the apparent grain development significantly reduced mechanical characteristics. [38]

TABLE II  
OVERLAYING AND CLADDING FOR DISSIMILAR METALS

Inconel alloy	Base metal	Process	Filler Material/ Interlayer	Ref
Inconel 617	AISI321	Brazing	AMS4772	[20]
Inconel 625	ASTM A516Gr.70	cladding	AWS5.14EQ-NiCrMo-3	[29]
Inconel 686	ASTM A516Gr.60	cladding	AWSERNiCrMo-14	[30]
Inconel 625	X-65 steel	Overlay	ErNiCrMo-3	[31]
Inconel 625	9%Ni steel	cladding	AWSErNiCrMo-3	[33]
Inconel 625	AISI4130	Overlay	ErNiCrMo-3	[34]
Inconel 625	CS	Overlay	Inconel 625	[35]
Inconel 625	ASTMA516 Grade70	Overlay	AWSErNiCrMo3 T1-4	[36]
Inconel 625	Q235A	Cladding	ErNiCrMo-3	[38]

Inconel 625	CS	Overlay	Inconel 625	[39]
-------------	----	---------	-------------	------

A study has been conducted on high temperature corrosion and electrochemical behavior of Inconel 625 weld overlay in PbSO<sub>4</sub>-Pb<sub>3</sub>O<sub>4</sub>-PbCl<sub>2</sub>-CdO-ZnO molten salt medium by E. Mohammadi Zahrani et al. After 24 hours in the molten salt medium, the SEM analysis showed that the most common types of corrosion attack were internal sulfidation and oxidation (especially at 800 and 700 degrees Celsius), interdendritic attack (observed at all temperatures), general surface corrosion (at all temperatures), void formation (at all temperatures), and a network of porous structure (at all temperatures) on the outermost layers and cross-sections of the corroded samples. Ni and Mo were more resistant to being diluted than the other key elements in the alloy 625 weld overlay, but Cr and Fe were very easy to dissolve in the molten salt media, which was found along with general surface corrosion. Despite Ni and Mo's notable resistance to dissolution, this was the reality. The protective Cr<sub>2</sub>O<sub>3</sub> layer flaked off of wrought alloy 625 (x = 0 and 5) and alloy 625 weld overlay (x = 10 and 5), but not alloy 625 weld cladding (corrosion rate = 0.52 0.17 mm/year) when subjected to 600 degrees Celsius and x = 10. [39-40]

Alireza Mirak et al. researched on dissimilar welding of Inconel 713 superalloy and AISI 4140 steel using Nd:YAG pulse laser. The mechanical and microscopic characteristics are being studied. A dendritic column formed towards the weld's edge as the temperature difference rose. However, at the center of the weld metal, a cellular dendritic structure began to form. The growth benefited from a rise in the temperature of the input heat. The weld metal's strength was severely reduced by the coarse dendritic structure. Hardness on the 4140 steel side increased as a function of heat input level due to the development of a martensitic microstructure in the heat-affected zone, while it remained relatively constant in the heat-affected zone of the Inconel 713 side. The brittle laves phase was formed and the tensile strength was decreased as a result of the rising heat input, which caused the elements Nb, Mo, and Ti to segregate in the interdendritic regions. Nevertheless, even with only 1875 J/mm of heat input, the welded connection reached its maximum tensile strength of 1068 MPa. Different levels of heat input caused the brittle fracture in the weld metal to become visible on the surface of the fracture in the tensile specimens. [41]

An assessment of microstructure and mechanical properties of inconel 601/304 stainless steel dissimilar weld done by Yahya Aghayar et al. In investigations using FE-SEM with a high vacuum, there was no evidence of segregation in the weld metal. A decrease in the amount of heat that was introduced resulted in an improvement of the mechanical characteristics of the welds as well as a significant refinement of the grain structure of the welds themselves. When these filler metal welds were welded using a pulsed current, the mechanical properties of the welds were improved to the greatest extent possible. Once everything was said and done, autogenous welding produced an

outstanding strength-ductility relationship (UTS = 485 MPa and elongation = 39%).. [42]

## II. CONCLUSION

From the literature review, it is possible to conclude the following.

1. Welding, cladding and overlaying are the most commonly used methods to combine Inconel with other alloys.
2. The most common techniques for welding Inconel and stainless steel together, which are two very different metals, are laser beam welding (LBW) and gas tungsten arc welding (GTAW/TIG)..
3. For overlaying Inconel, ErNiCrMo-3 filler wire seems to be the most widely accepted one.
4. The friction stir welding method was found to be more helpful in joining dissimilar alloys in the absence of filler material, narrow HAZ, lack of solidification effects, etc. Also, the process is environmentally clean.
5. Most research has been conducted on Inconel 718, Inconel 625, etc. The remaining Inconel alloys have undergone a comparatively smaller number of studies. There is a vast research gap with other Inconel alloys with higher grades, such as Inconel X-750 and above.

## References

- [1] DuPont J N, Lippold J C and Kiser S D, Welding metallurgy and weldability of Ni base alloys, Wiley, New Jersey (2009).
- [2] Johnson, W. A. "Properties and selection: nonferrous alloys and special-purpose materials." Molybdenum, Metals Handbook 2 (1990): 574.
- [3] M.J. Donachie, Superalloys: A Technical Guide, second ed., 2002, pp. 1–409. America (NY).
- [4] Derakhshi, Mohammad Amir, Jalal Kangazian, and Morteza Shamanian. "Electron beam welding of inconel 617 to AISI 310: Corrosion behavior of weld metal." Vacuum 161 (2019): 371-374
- [5] Mortezaie, A., and M. Shamanian. "An assessment of microstructure, mechanical properties and corrosion resistance of dissimilar welds between Inconel 718 and 310S austenitic stainless steel." International Journal of Pressure Vessels and Piping 116 (2014): 37-46.
- [6] Maurya, Anup Kumar, Chandan Pandey, and Rahul Chhibber. "Dissimilar welding of duplex stainless steel with Ni alloys: A review." International Journal of Pressure Vessels and Piping 192 (2021): 104439.
- [7] Kumar, Niraj, Chandan Pandey, and Prakash Kumar. "Dissimilar Welding of Inconel Alloys With Austenitic Stainless-Steel: A Review." Journal of Pressure Vessel Technology 145, no. 1 (2023): 011506.
- [8] Ajay, V., N. Kishore Babu, M. Ashfaq, T. Mahesh Kumar, and K. Vamsi Krishna. "A review on rotary and linear friction welding of Inconel alloys." Transactions of the Indian Institute of Metals (2021): 1-16.
- [9] Avery, Richard E. Pay attention to dissimilar-metal welds: guidelines for welding dissimilar metals. Toronto, ON, Canada: Nickel Development Institute, 1991.
- [10] Mortezaie, A., and M. Shamanian. "An assessment of microstructure, mechanical properties and corrosion resistance of dissimilar welds between Inconel 718 and 310S austenitic stainless steel." International Journal of Pressure Vessels and Piping 116 (2014): 37-46.
- [11] Vivek Patel, Akash Sali, James Hyder, Mike Corliss, David Hyder, and Wayne Hung. "Electron beam welding of inconel 718." Procedia Manufacturing 48 (2020): 428-435.
- [12] Thejasree, P., N. Manikandan, J. S. Binoj, K. C. Varaprasad, D. Palanisamy, and Ramesh Raju. "Numerical simulation and experimental investigation on laser beam welding of Inconel 625." Materials today: proceedings 39 (2021): 268-273.
- [13] Ahmad, Gulshad Nawaz, Mohammad Shahid Raza, N. K. Singh, and Hemant Kumar. "Experimental investigation on Ytterbium fiber laser butt welding of Inconel 625 and Duplex stainless steel 2205 thin sheets." Optics & Laser Technology 126 (2020): 106117.
- [14] Sharma, Sumit K., K. Biswas, A. K. Nath, I. Manna, and J. Dutta Majumdar. "Microstructural change during laser welding of Inconel 718." Optik 218 (2020): 165029.
- [15] Sivakumar, J., M. Vasudevan, and Nanda Naik Korra. "Systematic welding process parameter optimization in activated tungsten inert gas (A-TIG) welding of inconel 625." Transactions of the Indian Institute of Metals 73, no. 3 (2020): 555-569.
- [16] Prabakaran, S. Tamil, P. Sakthivel, Mohanraj Shanmugam, S. Satish, M. Muniyappan, and V. S. Shaisundaram. "Modelling and experimental validation of TIG welding of INCONEL 718." Materials Today: Proceedings 37 (2021): 1917-1931.
- [17] Rehman, Ateekh Ur, Yusuf Usmani, Ali M. Al-Samhan, and Saqib Anwar. "Rotary friction welding of inconel 718 to inconel 600." Metals 11, no. 2 (2021): 244.
- [18] Aghayar, Yahya, AmirReza Naghashzadeh, and Masoud Atapour. "An assessment of microstructure and mechanical properties of inconel 601/304 stainless steel dissimilar weld." Vacuum 184 (2021): 109970.
- [19] Sirohi, Sachin, Shailesh M. Pandey, Aleksandra Świerczyńska, Grzegorz Rogalski, Naveen Kumar, Michał Landowski, Dariusz Fydrych, and Chandan Pandey. "Microstructure and mechanical properties of combined GTAW and SMAW dissimilar welded joints between Inconel 718 and 304L austenitic stainless steel." Metals 13, no. 1 (2022): 14.
- [20] Paidar, M., KS Ashraff Ali, O. O. Ojo, V. Mohanavel, J. Vairamuthu, and M. Ravichandran. "Diffusion brazing of Inconel 617 and 321 stainless steel by using AMS 4772 Ag interlayer." Journal of Manufacturing Processes 61 (2021): 383-395.
- [21] Cheepu, Muralimohan, Y. Ashok Kumar Reddy, S. Indumathi, and D. Venkateswarlu. "Laser welding of dissimilar alloys between high tensile steel and Inconel alloy for high temperature applications." Advances in Materials and Processing Technologies 8, no. 2 (2022): 1197-1208.
- [22] Sahu, A. K., S. Bag, and Ke Huang. "Mitigation of micro-cracks in dissimilar welding of Inconel 718 and austenitic stainless steel." Philosophical Magazine Letters 100, no. 8 (2020): 365-374.
- [23] Corigliano, Pasqualino, and Vincenzo Crupi. "Fatigue analysis of Ti6Al4V/INCONEL 625 dissimilar welded joints." Ocean Engineering 221 (2021): 108582.
- [24] Srikanth, Sudhani, and A. Parthiban. "Microstructural analysis of Nd: YAG laser welding for Inconel alloy." Materials Today: Proceedings 21 (2020): 568-571.
- [25] Anuradha, M., Chittaranjan Das Vemulapalli, D. Venkateswaralu and Muralimohan Cheepu. "Microstructure Characterization in Dissimilar TIG Welds of Inconel Alloy 718 and High Strength Tensile Steel." Materials Science Forum: Vol. 969, pp 496-501 (2019): 1662-9752.
- [26] Anuradha, M., Vemulapalli Chittaranjan Das, P. Susila, Muralimohan Cheepu, and D. Venkateswarlu. "Microstructure and Mechanical Properties for the Dissimilar Joining of Inconel 718 Alloy to High-Strength Steel by TIG Welding." Transactions of the Indian Institute of Metals 73 (2020): 1521-1525.
- [27] Raj, Sanjay, and Pankaj Biswas. "Mechanical and microstructural characterizations of friction stir welded dissimilar butt joints of Inconel 718 and AISI 204Cu austenitic stainless steel." Materials Characterization 185 (2022): 111763.
- [28] Zhao, Xipeng, Xinjie Di, Xi Zhang, and Chengning Li. "Improvement in corrosion resistance of wire arc additive manufactured Inconel 625 alloy through heat treatment." Materials Research Express 8, no. 6 (2021): 066529.
- [29] Alvaraes, Camila P., Jorge CF Jorge, Luis FG de Souza, Leonardo S. Araujo, Matheus C. Mendes, and Humberto N. Farneze. "Microstructure and corrosion properties of single layer Inconel 625 weld cladding obtained by the electroslag welding process." Journal of Materials Research and Technology 9, no. 6 (2020): 16146-16158.



- [30] C.C. Silva, C.R.M. Afonso, A.J. Ramirez, M.F. Motta, H.C. Miranda, J.P. Farias, Assessment of microstructure of alloy Inconel 686 dissimilar weld claddings, *Journal of Alloys and Compounds* (2016), doi: 10.1016/j.jallcom.2016.05.231
- [31] Xu, Lianyong, Jianyang Zhang, Yongdian Han, Lei Zhao, and Hongyang Jing. "Insights into the intergranular corrosion of overlay welded joints of X65-Inconel 625 clad pipe and its relationship to damage penetration." *Corrosion Science* 160 (2019): 108169.
- [32] Xu, Lianyong, Chunsheng Shao, Lei Tian, Jianli Zhang, Yongdian Han, Lei Zhao, and Hongyang Jing. "Intergranular corrosion behavior of Inconel 625 deposited by CMT/GTAW." *Corrosion Science* 201 (2022): 110295.
- [33] FranciscoWerley Cipriano Farias, Joao da Cruz Payao Filho and Luiz Mauricio Barreto de Azevedo. "Microstructural and Mechanical Characterization of the Transition Zone of 9%Ni Steel Cladded with Ni-Based Superalloy 625 by GTAW-HW." *Metals* 8-1007 (2019): doi:10.3390.
- [34] Guo, Longlong, Zheng Hualin, Liu Shaohu, Li Yueqin, Xu Xiaodong and Feng Chunyu. "Formation Quality Optimization and Corrosion Performance of Inconel 625 Weld Overlay Using Hot Wire Pulsed TIG." *Rare Metal Materials and Engineering*, (2016): 45(9): 2219-2226.
- [35] P. Elango and S. Balaguru." Welding Parameters for Inconel 625 Overlay on Carbon Steel using GMAW ". *Indian Journal of Science and Technology*, Vol 8(31), (2015) 84309
- [36] Alvaraes, Camila P., Francisco Carlos Albuquerque Madalena Jorge CF Jorge, Luis FG de Souza, Leonardo S. Araujo, Matheus C. Mendes, and Humberto N. Farneze. "Performance of the INCONEL 625 alloy weld overlay obtained by FCAW process." *Revistamateria* V24, no.1 (2019): 1517-7076
- [37] Pavan Kumar Korrapati, Vaibhav Krishna Avasarala, Movva Bhushan, K. Devendranath Ramkumar, N. Arivazhagan N, S. Narayanan." Assessment of Mechanical properties of PCGTA weldments of Inconel 625". *Procedia Engineering* 75 ( 2014 ) 9 – 13
- [38] Fujia Xu a, Yaohui Lv c, Yuxin Liuc, Binshi Xub,c and Peng Heb. "Effect of heat treatment on microstructure and mechanical properties of Inconel 625 alloy fabricated by pulsed plasma arc deposition". *Physics Procedia* 50 ( 2013 ) 48 – 54
- [39] Zahrani, E. Mohammadi, and A. M. Alfantazi. "High temperature corrosion and electrochemical behavior of INCONEL 625 weld overlay in PbSO<sub>4</sub>-Pb<sub>3</sub>O<sub>4</sub>-PbCl<sub>2</sub>-CdO-ZnO molten salt medium." *Corrosion Science* 85 (2014) 60-76.
- [40] Zahrani, E. Mohammadi, and A. M. Alfantazi. "Hot corrosion of Inconel 625 wrought alloy and weld overlay on carbon steel by gas metal arc welding in 47 PbSO<sub>4</sub>-23 ZnO-13 Pb<sub>3</sub>O<sub>4</sub>-7 PbCl<sub>2</sub>-5 CdO-5 Fe<sub>2</sub>O<sub>3</sub> molten salt mixture." *Corrosion Science* 183 (2021): 109348.
- [41] Mirak, Alireza, Behrooz Shams, and Soroush Bakhshi. "Dissimilar welding of Inconel 713 superalloy and AISI 4140 steel using Nd: YAG pulse laser: An investigation on the microstructure and mechanical properties." *Optics & Laser Technology* 152 (2022): 108143.
- [42] Aghayar, Yahya, AmirReza Naghashzadeh, and Masoud Atapour. "An assessment of microstructure and mechanical properties of inconel 601/304 stainless steel dissimilar weld." *Vacuum* 184 (2021): 109970.